Centrin4 coordinates cell and nuclear division in *T. brucei*

Jie Shi[1], Joseph B. Franklin[2], Jordan T. Yelinek[2], Ingo Ebersberger[3,4], Graham Warren[2,*] and Cynthia Y. He[2,‡,§]

[1]Department of Biological Sciences, National University of Singapore, 14 Science Drive 4, Singapore 117543
[2]Department of Cell Biology, Yale University School of Medicine, 333 Cedar Street, New Haven, CT 06520, USA
[3]Centre for Integrative Bioinformatics Vienna, Max F. Perutz Laboratories, Dr Bohr-Gasse 9, A-1030 Vienna, Austria
[4]University of Veterinary Medicine, Veterinärplatz 1, 1210 Vienna, Austria
*Present address: Max F. Perutz Laboratories, Dr Bohr-Gasse 9, A-1030 Vienna, Austria
‡Present address: Department of Biological Sciences, National University of Singapore, 14 Science Drive 4, Singapore 117543
§Author for correspondence (e-mail: dbshyc@nus.edu.sg)

Accepted 2 July 2008
Journal of Cell Science 121, 3062-3070 Published by The Company of Biologists 2008
doi:10.1242/jcs.030643

Summary

Centrins are Ca^{2+}-binding proteins that have been implicated in a number of biological processes, including organelle duplication, mRNA export, DNA repair and signal transduction. In the protozoan parasite *Trypanosoma brucei* we have previously described *Tb*Centrin2, which is present on a bi-lobed structure, and involved in the duplication and segregation of the Golgi complex. Recently, another centrin, *Tb*Centrin4, was also found at the bi-lobe and has been implicated in organelle segregation and cytokinesis. We now show that cytokinesis is not inhibited, but that a dysregulation of nuclear and cell division leads to the production of zoids – daughter siblings that contain all organelles except the nucleus. Our results, therefore, suggest that *Tb*Centrin4 is involved in processes that coordinate karyokinesis and cytokinesis.

Supplementary material available online at
http://jcs.biologists.org/cgi/content/full/121/18/3062/DC1

Key words: *Trypanosoma brucei*, Centrin, Basal body, Golgi, Cell division, Zoid

Introduction

Centrins are highly conserved components of centrosomes, such as microtubule-organizing centers and basal bodies (Salisbury 1995; Chapman et al., 2000). Centrins are key regulators for the normal function and duplication of these structures (Baum et al., 1986; Middendorp et al., 2000; Salisbury, 2002; Paoletti et al., 2003; Selvapandiyan et al., 2004), and are also required for a variety of other cellular processes including DNA repair, mRNA export and signal transduction (Araki et al., 2001; Wolfrum et al., 2002; Fischer et al., 2004). Although this variety of functions can be achieved by a single centrin gene in organisms such as *Saccharomyces cerevisiae*, multiple centrin genes have been found in many other organisms, including mammals. Structural analyses suggest different biochemical properties for different centrin isoforms (Hu and Chazin, 2003; Sheehan et al., 2006; Yang et al., 2006) and different intracellular localizations and functions have also been reported (Giessl et al., 2004; Ruiz et al., 2005; Hu et al., 2006; Gogendeau et al., 2008).

In *Trypanosoma brucei*, the causative agents of African sleeping sickness, we have identified previously five putative centrins in the completed genome (He et al., 2005). Only *Tb*Centrin1 and *Tb*Centrin2 are recognized by 20H5, a monoclonal antibody originally raised against centrin from *Chlamydomonas reinhardtii* (Salisbury et al., 1988). Both of these two centrins are present on the basal bodies that nucleate the flagellum required for cell locomotion, and are required for basal body duplication. *Tb*Centrin2, however, is additionally present on a bi-lobed structure that is closely associated with the single Golgi stack in this parasite. Duplication of the bi-lobed structure and duplication of the Golgi complex are highly coordinated during the cell cycle and depletion of *Tb*Centrin2 protein by inducible RNA interference (RNAi) leads to the inhibition of Golgi duplication, suggesting a role for the bi-lobed structure in Golgi biogenesis. Depletion of *Tb*Centrin2 also inhibits segregation of the kinetoplast (the mitochondrial DNA aggregate to which the basal bodies are attached) and cell division. It does not, however, inhibit nuclear division so that large multinucleated cells accumulate (He et al., 2005).

Here, we characterize another *T. brucei* centrin, *Tb*Centrin4, which is not recognized by the 20H5 antibody but, nevertheless, is associated with the bi-lobed structure marked by *Tb*Centrin2. The bi-lobe association of this centrin [also named TbCen1 (Selvapandiyan et al., 2007)] has recently been reported by Selvapandiyan and colleagues, who used GFP-fusion constructs and hemagglutinin (HA) tagging (Selvapandiyan et al., 2007). Their data suggested that *Tb*Centrin4 is involved in the segregation of duplicated organelles, depletion of which leads to inhibition of cell division. Our data, however, suggest that organelle segregation and cell division occur normally. The segregation of nuclei and/or its coordination with cytokinesis appear to be affected, leading to the production of anucleated daughter cells termed zoids.

Results

Phylogenetic analyses of *Tb*Centrin4

Unlike other centrins, but similar to calmodulins, *Tb*Centrin4 contains a very short N-terminal extension sequence upstream of the Ca^{2+}-binding EF-hand domains (supplementary material Fig. S1). Furthermore, it was not recognized on immunoblots when using the monoclonal antibody 20H5 (Fig. 1A), which was raised against the *C. reinhardtii* centrin, and had been shown to cross-react with centrins from a variety of organisms. This might reflect the lack of a ten amino acid (aa) long epitope (EIxxAFxLFD) that has been identified as being necessary for the recognition by 20H5 (Klotz et al., 1997).

To further understand how *Tb*Centrin4 is related to the centrins that have been identified in other organisms, a phylogenetic analysis

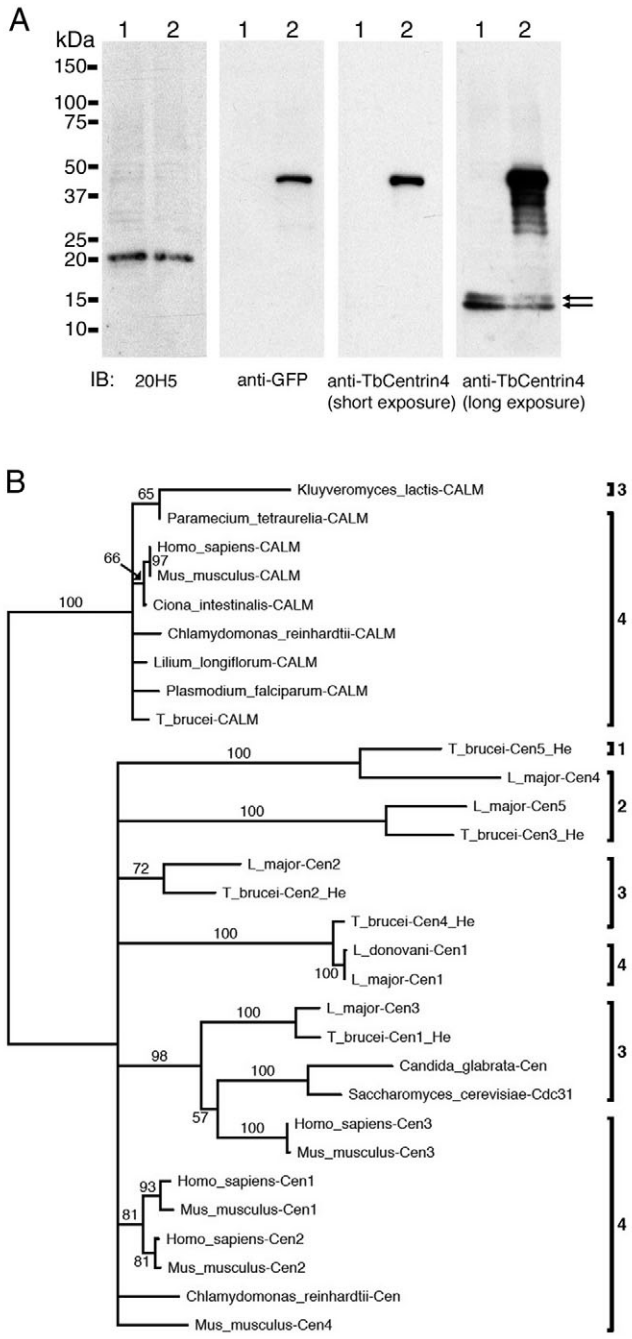

Fig. 1. Characterization of *Tb*Centrin4. (A) Characterization of antibodies against *Tb*Centrin4. Total lysates containing equal amounts of protein (12 µg) from control procyclic cells (lanes labeled 1) or cells stably expressing *Tb*Centrin4-YFP (lanes labeled 2) were fractionated, separated by electrophoresis and immunoblotted with the indicated antibodies. Note that antibody against GFP (which also recognizes YFP; second panel) recognized the same fusion protein as polyclonal antibodies against *Tb*Centrin4 (third panel), which also recognized two proteins at ~14 and 16 kDa (arrows, fourth panel, longer exposure of third panel). These represent endogenous *Tb*Centrin4 and were not recognized by the monoclonal antibody 20H5 (which recognizes co-migrating *Tb*Centrin1 and *Tb*Centrin2; first panel). (B) Maximum-likelihood sequence tree of centrins and calmodulins. Numbers on branches represent bootstrap support values. Branches supported by less than 50% of the bootstrap replicates were collapsed to form a multifurcation. L_major, *Leishmania major*; L_donovani, *Leishmania donovani*; CALM, calmodulin; Cen, centrin. We used the centrin nomenclature suggested by Selvapandiyan et al. (Selvapandiyan et al., 2007) with the exception of the *Tb*Centrins (He et al., 2005), which are suffixed '_He' to highlight our results. The numbers on the right indicate the number of predicted EF-hand domains in those proteins grouped by the numbered square brackets.

of centrins and calmodulins from various organisms (Table 1) was performed using a maximum-likelihood method (Fig. 1B). All calmodulins in our data set formed a distinct and highly supported clade, indicating a common ancestor that is different to the centrins. A second strongly supported clade was formed by the Cdc31-type centrins (Bornens and Azimazadeh, 2007). The presence of animal, fungi and protist sequences in this clade indicates an early origin of these proteins in eukaryotic evolution, possibly from an ancestral protein, shared with no other centrin in our data set. For the remaining centrins, only the very recent evolutionary history of the individual proteins is resolved, making it difficult to draw any conclusion concerning the phylogenetic relationships of protist and mammalian centrins, apart from the Cdc31-like subfamily.

We next considered the number of EF-hand domains (SMART accession number SM00054) predicted in the individual centrins as a possible criterion for their classification (Selvapandiyan et al., 2007). Eigtheen of the 30 proteins analyzed, including all but one calmodulin, contained four EF-hand domains in conserved positions (supplementary material Fig. S1). Parsimony suggests that this situation corresponds to the ancestral state. The remaining proteins contain one, two, or in the case of *Tb*Centrin4, three EF-hand domains. Sequences with differing numbers of EF-hand domains are present in the same well-supported clades, suggesting that loss of EF-hand domains must have occurred several times

Table 1. Centrins and calmodulins used for phylogenetic analyses

	Gene (as shown in Fig. 1B)	Accession number
Calmodulins	Chlamydomonas_reinhardtii-CALM	P04352
	Ciona_intestinalis-CALM	O02367
	Homo_sapiens-CALM	P62158
	Kluyveromyces_lactis-CALM	O60041
	Lilium_longiflorum-CALM	P62201
	Mus_musculus-CALM	P62204
	Paramecium_tetrauralia-CALM	P07463
	Plasmodium_falciparum-CALM	P24044
	Trypanosoma_brucei-CALM	Tb11.01.4624
Centrins	Candida_glabrata-Cen	XP448610.1
	Chlamydomonas_reinhardtii-Cen	P05434.1
	Homo_sapiens-Cen1	AH29515.1
	Homo_sapiens-Cen2	NP004335.1
	Homo_sapiens-Cen3	O15182.2
	L_donovani-Cen1	AAL01153.1
	L_major-Cen1	XP001683292.1
	L_major-Cen2	XP001680978.1
	L_major-Cen3	XP001686337.1
	L_major-Cen4	XP001685381.1
	L_major-Cen5	XP001687199.1
	Mus_musculus-Cen1	NP031619.3
	Mus_musculus-Cen2	NP062278.2
	Mus_musculus-Cen3	AAH54097.1
	Mus_musculus-Cen4	CAI26236.1
	Saccharomyces_cerevisiae-Cdc31	NP014900.1
	T_brucei-Cen1_He	Tb927.4.2260
	T_brucei-Cen2_He	Tb927.8.1080
	T_brucei-Cen3_He	Tb10.6k15.1830
	T_brucei-Cen4_He	Tb927.7.3410
	T_brucei-Cen5_He	Tb11.01.5470

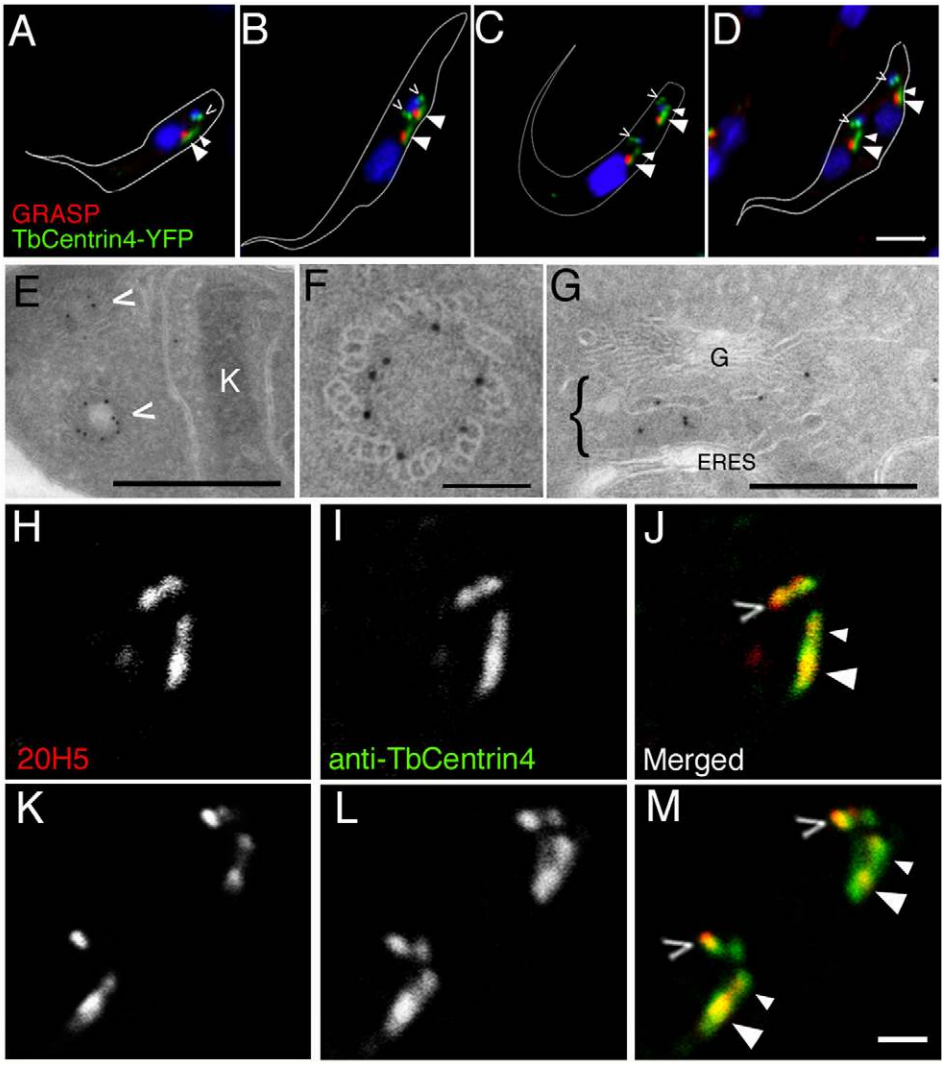

Fig. 2. Localization of *Tb*Centrin4. (A-D) Cells stably expressing *Tb*Centrin4-YFP (green) were fixed and labeled for Golgi (anti-GRASP; red), kinetoplasts (DAPI; small blue dots) and nuclei (DAPI; large blue structures). The outline of each cell is indicated by a white line. Note the presence of *Tb*Centrin4 on both basal bodies (open arrowheads) and the bi-lobe structure (filled arrowheads; large arrowheads indicate the lobe next to the old Golgi, small arrowheads the lobe that becomes associated with the new Golgi), which was closely associated with the Golgi throughout the cell cycle, as previously observed for *Tb*Centrin2. The same cells are shown at higher magnification in supplementary material Fig. S2. (E-G) *Tb*Centrin4-YFP cells were also fixed for cryo-iEM and labeled with an anti-GFP antibody followed by protein-A–gold (10 nm) labeling. *Tb*Centrin4 was found at both the basal bodies (indicated by open arrowheads in E; shown also in F) and the Golgi/ERES region (bracketed region in G). K, kinetoplast; G, Golgi; ERES, ER export site. (H-M) Representative confocal images of a 1K1N (cell containing one kinetoplast and one nucleus) (H-J) and a 2K2N cell (containing duplicated kinetoplasts and nuclei) (K-M) representing early and late cell cycle stages showing that 20H5 (H,K) and anti-*Tb*Centrin4 (I,L) both label basal bodies (open arrowheads) and the bi-lobe structure (filled arrowheads). Scale bars, 5 μm (A-D); 0.5 μm (E,G); 0.2 μm (F); 1 μm (H-M).

and independently during the evolution of these proteins. As a consequence, neither the presence nor the absence of particular EF-hand domains in the individual centrins helped in centrin classification.

Recently, Selvapandiyan et al. have suggested that *Tb*Centrin4 should be renamed to *Tb*Cen1 to reflect its similarity to mammalian centrin1 (Selvapandiyan et al., 2007). In light of the present analyses, it would seem to be reasonable to keep the original nomenclature, to avoid unnecessary confusion, and to change it only when there is more information concerning the molecular origin of *Tb*Centrin4.

Antibodies against *Tb*Centrin4

To obtain *Tb*Centrin4-specific antibodies, the full-length coding sequence was fused to a 6xHis reporter and the purified fusion protein used for raising polyclonal antibodies in rabbits. The affinity-purified antibody recognized a pair of bands at ~14 kDa and 16 kDa in the control cell lysates (Fig. 1A; fourth panel, long exposure), which corresponded to the theoretical molecular size of *Tb*Centrin4, but were much smaller than the size of *Tb*Centrin1 (~21 kDa), *Tb*Centrin2 (~21 kDa), *Tb*Centrin3 (~19 kDa) and *Tb*Centrin5 (~21 kDa) (Fig. 1A; first panel, 20H5). This antibody also recognized an ~43 kDa band in cells expressing a *Tb*Centrin4-YFP fusion protein (Fig. 1A; third panel, short exposure), but not other *Tb*Centrins fused to YFP (data not shown). It is not yet clear whether the doublet represents post-translational modifications to the *Tb*Centrin4 protein. Depletion of *Tb*Centrin4 in RNAi experiments led to decreased levels of both bands (see below, Fig. 3B).

*Tb*Centrin4 is present on the bi-lobed structure

To examine the intracellular localization, cells stably expressing the *Tb*Centrin4-YFP fusion were fixed and co-labeled for the Golgi matrix marker GRASP (He et al., 2004). Similar to *Tb*Centrin2 (He et al., 2005), *Tb*Centrin4-YFP labeled a Golgi-associated, bi-lobed structure in addition to the basal bodies. At the beginning of a cell cycle, a single Golgi stack was found to be associated with one lobe of the bi-lobed structure (Fig. 2A). Later, a new Golgi stack appeared next to the old one, which was associated with the other more-posterior lobe of the bi-lobe (Fig. 2B). As the new Golgi grew and increasingly separated from the old Golgi, the bi-lobe structure also underwent duplication and separation (Fig. 2C), each maintaining its association with one of the Golgi stacks during the rest of the cell cycle (Fig. 2D).

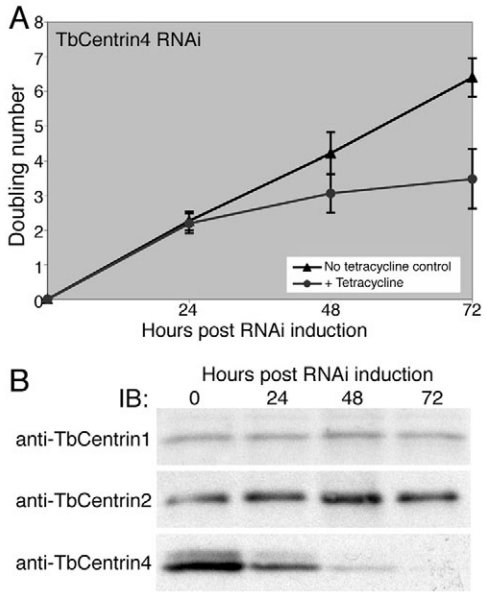

Fig. 3. Depletion of *Tb*Centrin4 inhibits cell growth. (A,B) Cells with a stably integrated Centrin4-RNAi construct were grown with tetracycline to induce RNAi or without. Samples were taken for cell counting (A; results are given as the mean ± s.d., *n*=3) and immunoblotting (B) using the indicated antibodies to confirm selective depletion of *Tb*Centrin4, but not *Tb*Centrin1 and *Tb*Centrin2. 12 μg total protein were loaded in each lane.

*Tb*Centrin4-YFP cells were then fixed for immuno-gold labeling of cryo-EM sections. Basal bodies are readily identified by their characteristic 9+0 microtubule arrangement, and gold-labeling of *Tb*Centrin4-YFP was found around the inside rim of the cylindrical profiles (open arrowheads in Fig. 2E and F). The bi-lobe, by contrast, does not appear to have such a clearly defined morphology at the ultra-structural level. However, earlier work has shown that *Tb*Centrin2 is present in the region occupied by the ER export site (ERES), the cis-Golgi network (CGN) and the intervening region (He et al., 2005). Labeling for *Tb*Centrin4 recapitulated this labeling pattern (Fig. 2G).

Colocalization of *Tb*Centrin4 with *Tb*Centrin2 was detected by confocal microscopy on cells double-labeled with anti-*Tb*Centrin4 and 20H5 antibodies (Fig. 2H-M). Although the staining intensity varied between *Tb*Centrin2 and *Tb*Centrin4 on different parts of the basal bodies and the bi-lobe, both *Tb*Centrins were clearly associated with these same structures, and the staining patterns largely overlapped. The deduced aa sequence of *Tb*Centrin4 shows 35.7% identity to that of *Tb*Centrin2, but it is unlikely that the bi-lobe labeling with anti-*Tb*Centrin4 antibody represented weak crossreactivity with *Tb*Centrin2, because anti-*Tb*Centrin4 antibody did not react with *Tb*Centrin2 on immunoblots (see Fig. 1A). In addition, immunofluorescence labeling of the basal bodies and also the bi-lobe with anti-*Tb*Centrin4 antibodies was competed with purified GST-tagged *Tb*Centrin4 but not *Tb*Centrin2 (supplementary material Fig. S3).

*Tb*Centrin4 depletion leads to the formation of zoids

Depletion of *Tb*Centrin2 has been previously shown to inhibit Golgi duplication, suggesting a role for the bi-lobed structure in Golgi biogenesis (He et al., 2005). The presence of *Tb*Centrin4 in the same structure raised the possibility that it is also involved in the same process. To test this, *Tb*Centrin4 was depleted in inducible RNAi experiments, and parasite numbers was monitored at 24, 48 and 72 hours post induction. Until 24 hours post-induction with tetracycline, the cells grew at the same rate as un-induced control cells. Cell duplication then slowed and cell growth became completely arrested at 72 hours post induction (Fig. 3A). This growth pattern was very similar to that reported recently (Selvapandiyan et al., 2007), although arrest, in our hands, occurred more than 24 hours earlier. This was not the result of using higher concentrations of tetracycline (10 μg/ml), because the same results were obtained when RNAi was induced at 1 μg/ml or 0.2 μg/ml (supplementary material Fig. S4A).

Specific depletion of *Tb*Centrin4 protein was confirmed by immunoblotting of whole-cell lysates obtained at the different time points post induction. Whereas the levels of *Tb*Centrin1 and *Tb*Centrin2 remained unchanged, the levels of the *Tb*Centrin4 doublet decreased over time to <5% at 72 hours (Fig. 3B). Similar depletion kinetics were observed when 1 μg/ml or 0.2 μg/ml tetracycline were used in RNAi experiments (supplementary material Fig. S4B).

*Tb*Centrin4-RNAi cells at different times post induction were then fixed and stained with DAPI to examine their DNA content (see Materials and Methods), and these results were compared to those for *Tb*Centrin2-RNAi cells (Fig. 4A,B). The control (un-induced) populations showed a similar distribution, with ~80% of cells containing one nucleus and one kinetoplast (1K1N cells), 5-8% of cells containing one nucleus and duplicated kinetoplasts (2K1N cells), and 5-10% of cells containing duplicated kinetoplasts as well as nuclei (2K2N cells). All other cell variations, including multinucleated cells, were considered abnormal, and these constituted <3% of the control populations. Upon induction, the number of normal cells, in particular the 1K1N cells, decreased in both *Tb*Centrin2 and *Tb*Centrin4-RNAi cells. The persistence of some normal cells, even 48 and 72 hours post induction, might be owing to incomplete *Tb*Centrin depletion (Fig. 3B; supplementary material Fig. S4B). To test this, *Tb*Centrin4-RNAi cells were stained with anti-*Tb*Centrin4 antibodies at different time points. The vast majority of cells (>95%) lacked staining of *Tb*Centrin4 irrespective of their DNA content. The little basal body and bilobe staining that was detected, was only present in normal cells (1K1N, 2K1N and 2K2N; supplementary material Fig. S5) and might have derived from RNAi revertants (cells that became non-responsive to RNAi during prolonged cultivation) (Chen et al., 2003).

In both *Tb*Centrin2-RNAi and *Tb*Centrin4-RNAi cell populations, there was also an accumulation of abnormal cells, in particular of multinucleated cells and of cells that contained two nuclei and a single kinetoplast (1K2N cells). In the case of *Tb*Centrin2-RNAi cells, this is probably due to inhibition of basal body duplication, which is required for kinetoplast segregation (Robinson and Gull, 1991). Cell division is also inhibited, although nuclear division continues, explaining the initial appearance of 1K2N cells and the later accumulation of multinucleated cells (He et al., 2005).

In the case of *Tb*Centrin4-RNAi cells, the explanation for the increase in 1K2N and mutinucleated cells appears to be different. This arises from the observation that there was also a rapid accumulation of zoids – cells lacking a nucleus. These zoids constituted ~10% of the cell population at 24 hours post induction, ~25% at 48 hours post induction and >40% at 72 hours post induction (Fig. 4B). Again, a similar accumulation of zoids was observed in experiments in which RNAi was induced by only 1

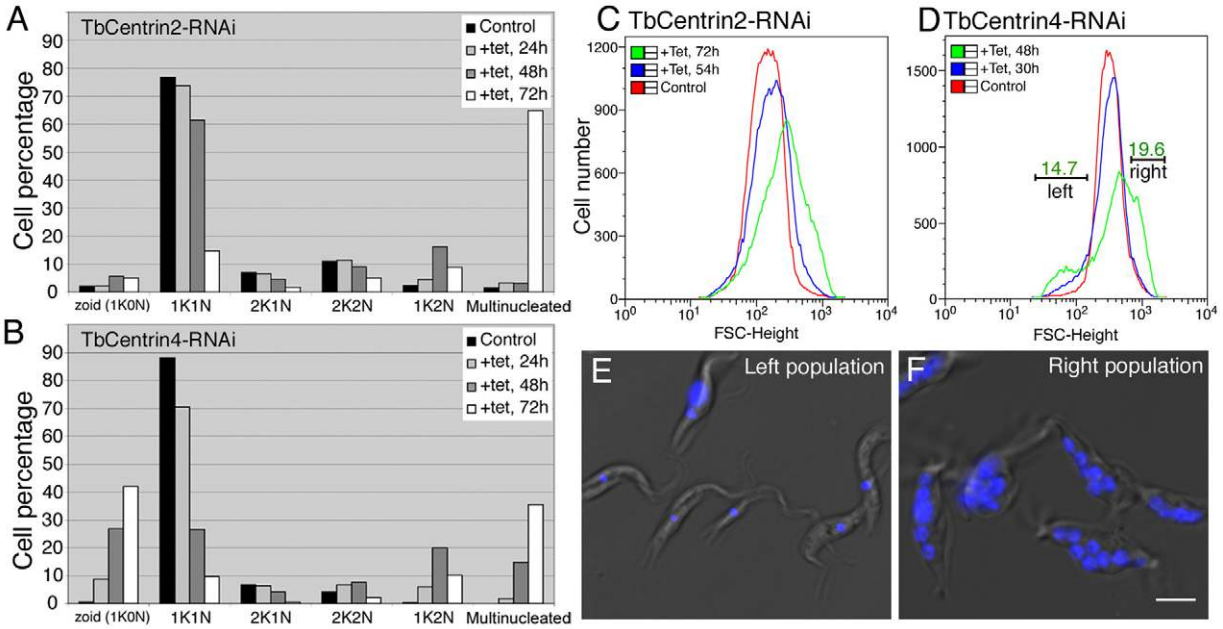

Fig. 4. Generation of zoids through depletion of *Tb*Centrin4, but not *Tb*Centrin2. (A,B) Cells were induced for *Tb*Centrin2-RNAi (A) or *Tb*Centrin4-RNAi (B), and the DNA content of fixed cells was monitored using DAPI staining. Cells were divided into six categories: one kinetoplast and no nucleus (1K0N; zoids), one kinetoplast and one nucleus (1K1N), two kinetoplasts and one nucleus (2K1N), two kinetoplasts and two nuclei (2K2N), one kinetoplast and two nuclei (1K2N), and cells with multiple nuclei (Multinucleated). Results from two independent experiments were averaged for n=500 cells/time point. The number of zoids (1K0N) increased in cells depleted of *Tb*Centrin4 but not of *Tb*Centrin2. (C,D) Cells analyzed by flow cytometry using forward scatter to measure the cell size. 100,000 events were analyzed for each time point. (E,F) *Tb*Centrin2-depletion led to larger cells, whereas depletion of *Tb*Centrin4 generated two populations, the smaller cells mostly zoids (E), the larger cells mostly multinucleated (F). Scale bar, 5 μm.

μg/ml tetracycline (supplementary material Fig. S4C). This rapid increase in zoids was not observed in *Tb*Centrin2-RNAi cells throughout the course of induction, as confirmed by size measurements of *Tb*Centrin2 and *Tb*Centrin4-RNAi cells at various time points post induction (Fig. 4C,D). The forward scatter was used to monitor cell size. During induction of RNAi, the average forward scatter of *Tb*Centrin2-RNAi populations became increasingly bigger (Fig. 4C), suggestive of increasing cell size. This is consistent with the observation that cytokinesis is inhibited in these cells and multinucleated cells accumulate over time (He et al., 2005). By marked contrast, the *Tb*Centrin4-RNAi cells split into two populations, one with larger and the other with smaller cells (Fig. 4D). The largest 20% (right population) and smallest 15% (left population) of cells were isolated and fixed for fluorescence microscopy (Fig. 4E,F). Whereas the right cell population contained mostly multinucleated cells (>90%; n=500 cells), the left population was highly enriched in zoids (~80%; n=500 cells).

Furthermore, in *Tb*Centrin4-RNAi parasites, cells that were in the final stages of cell division could be found, with two daughter cells connected only at the extreme posterior ends or recently separated (Fig. 5A,B). One daughter cell inherited two nuclei and one kinetoplast, becoming a 1K2N cell; the other inherited only a single kinetoplast and became a zoid, suggesting that the zoids and 1K2N cells were produced as siblings. Despite the unequal inheritance of the nuclei, the 1K2N and zoid daughters appeared to inherit all other organelles equally, including the kinetoplasts (Fig. 5A,B), the basal bodies, the bi-lobe and the Golgi (Fig. 5C,D) as well as all other organelles examined (mitochondria, lysosomes, ERES and flagella; data not shown).

To determine whether kinetoplast duplication and unequal nuclear segregation continued to occur at late stages of *Tb*Centrin4-RNAi induction, the K:N ratio (number of kinetoplasts divided by number of nuclei in each cell) was calculated at 48 and 72 hours post induction in 100 multi-nucleated cells. In normal cells, the K:N ratio is between 1 and 2 because the kinetoplast replicates and divides earlier than the nucleus. However the value of the K:N ratio decreased to 0.44±0.19 in the multinucleated cells at 48 hours and to 0.37±0.15 at 72 hours post induction. This suggests inhibition of kinetoplast duplication and/or segregation at these late stages or further unequal division of multinucleated cells to produce zoids, or both.

Depletion of *Tb*Centrin4 does not affect cytokinesis

In *T. brucei*, the nucleus is the last organelle to complete division before cytokinesis begins (Sherwin and Gull, 1989; Robinson et al., 1995). Cell division initiates at the anterior tip of the cell and moves along the long axis of the cell body, partitioning all duplicated and segregated organelles into each daughter cell. The flagellum attachment zone (FAZ), which is a complex microtubule-containing cytoplasmic structure that mediates flagellum attachment to the cell body (Sherwin and Gull, 1989), has been proposed to have an important role by determining the formation of the cytokinetic furrow (Robinson et al., 1995; Vaughan et al., 2008).

The importance of FAZ in cell division raised the possibility that the generation of the 1K2N cell and the zoid in *Tb*Centrin4-depleted cells are the result of a defect in formation or placement of the FAZ. To test this, *Tb*Centrin4-RNAi cells were fixed and stained with L3B2, a monoclonal antibody that labels the FAZ (Kohl et al., 1999). FAZs were found in all cell categories including 1K2N cells and zoids (Fig. 6C,D), suggesting normal segregation of duplicated FAZ. Furthermore, although zoids are thinner than normal 1K1N cells, the average length of the FAZ in zoids was very similar to that in

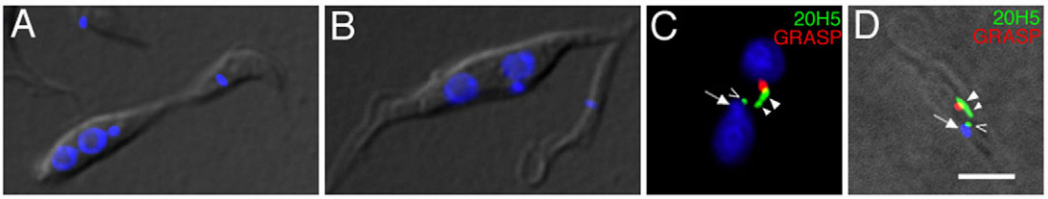

Fig. 5. Zoids and 1K2N cells appear to be produced as siblings. Cells induced for *Tb*Centrin4-RNAi for 24 hours were fixed and labelled with DAPI (nucleus, kinetoplast), 20H5 (basal bodies and bi-lobe) and anti-GRASP (Golgi). (A) A cell near the end of cytokinesis, separating into one daughter cell that contains two nuclei, and the other daughter cell without a nucleus. (B) A cell just after division, one daughter cell with two nuclei, the other with none. (C,D) Both siblings contain basal bodies (open arrowheads), a kinetoplast (arrows), a bi-lobe (closed arrowheads; the large arrowhead indicating the lobe that is associated with the single Golgi stack, the small arrowhead indicating the other lobe) and a Golgi complex (red). Scale bar, 5 µm.

1K1N cells (Fig. 6E), suggesting normal duplication and formation of this important structure in cells depleted of *Tb*Centrin4. Consistent with this, the flagella remained attached to the cell bodies in the majority of cells until 48 hours post induction. Afterwards, partial detachment was observed in some cells at which point the cell morphology was grossly perturbed and cell division was completely arrested (supplementary material Fig. S6).

Interestingly, unlike in normally dividing cells in which cell division only initiates after full segregation of the nuclei, cell division in many *Tb*Centrin4-RNAi cells found at 24-48 hours post induction appeared to occur before full segregation of the duplicated nuclei (compare Fig. 6F,G with Fig. 6A,B). This was evident, for example, in Fig. 6F, where the daughter cell that contained a normal looking new FAZ (marked by triple arrows) had already separated partially from the other daughter before full segregation of the duplicated nuclei, leading to the formation of a 1K2N cell and a zoid (Fig. 6G).

As a comparison, the 1K2N cells generated by *Tb*Centrin2-RNAi were also examined for FAZ labeling to test whether inhibition of cytokinesis in these cells was due to inhibition of FAZ. As expected, >70% of these cells contained only one FAZ that appeared normal. The others contained a second, more posterior staining for FAZ, but this new FAZ stump often appeared aborted or malformed (Fig. 6H,I). Interestingly, formation of the new flagellum was consistently observed in these cells. Without associated new FAZ, these new flagella were not attached to the cell body (see Fig. 6H).

The relationship between the FAZ and the bi-lobe was also investigated in control cells. As shown in Fig. 7, the posterior end of the FAZ was partially embedded in the anterior end of the bi-lobe at all stages of the cell cycle.

Discussion

The kinetoplastida parasite, *T. brucei*, contains a unique form of centrin, termed *Tb*Centrin4 (He et al., 2005) or TbCen1 (Selvapandiyan et al., 2007). The deduced 149 aa sequence lacks a distinct N-terminal extension that was thought to be a feature distinguishing centrins from calmodulins (Friedberg, 2006). However, extensive phylogenetic analyses do not support its grouping with calmodulins. Neither does it group strongly with any of the four types of mammalian centrins identified so far (Friedberg, 2006). The phylogenetic analysis of centrins by Selvapandiyan et al. was performed using the UPGMA method, which is a distance-based clustering algorithm only applicable when all sequences in the data have evolved according to the same molecular clock (Selvapandiyan et al., 2007). If this assumption is violated, UPGMA is known to retrieve the wrong trees (Page and Holmes, 2004). A clock test was therefore performed on the same centrin data set and the hypothesis of a clock-like evolution was rejected for these sequences. It is, therefore, premature to rename *Tb*Centrin4 TbCen1 because this makes the misleading suggestion that *Tb*Centrin4 is phylogenetically more related to mammalian centrin1 (CETN1). Renaming must await more information as to the molecular origin of *Tb*Centrin4.

As with the previously characterized *Tb*Centrin2, *Tb*Centrin4 was found on the basal bodies as well as a bi-lobed structure closely associated with the single Golgi complex in *T. brucei* cells early in

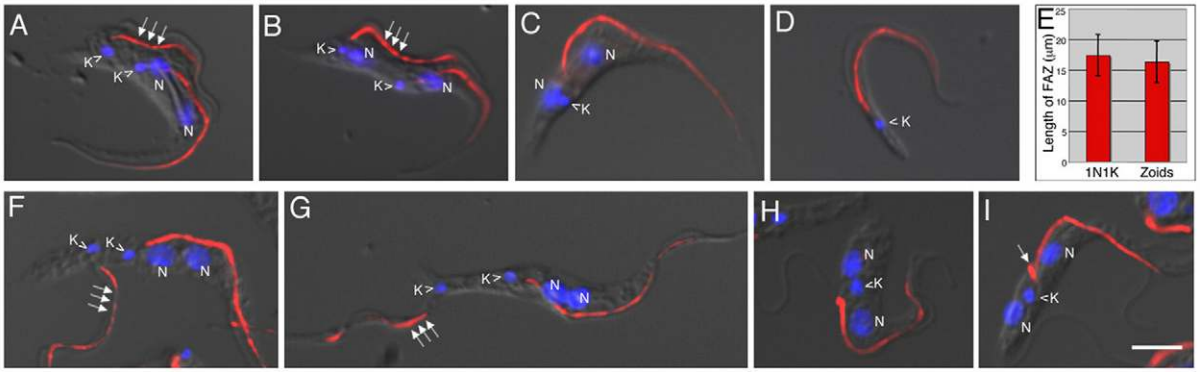

Fig. 6. (A-I) Duplication of the FAZ is unaffected by depletion of *Tb*Centrin4. Control (A,B), *Tb*Centrin4-RNAi (C-G) and *Tb*Centrin2-RNAi (H,I) cells were fixed and labeled for FAZ (L3B2; red) and DNA (DAPI; blue). Note that the new FAZ (indicated by triple arrows) in control cells that undergo nuclear division remained attached to the cell body and that cell division initiated only after full segregation of the duplicated nuclei (distance ~6 µm ; not shown) (see also Robinson et al.,1995). In cells depleted of *Tb*Centrin4 (C,D), the FAZ was the same length in both the 1K1N (control) and 1K0N (zoid) cells (E; *n*=100, mean ± s.d.). However, cell division initiated even before full segregation of the nuclei (F,G). By contrast, in cells depleted of *Tb*Centrin2, formation of the new FAZ was inhibited (truncated new FAZ indicated by arrow), consistent with the known inhibition of cytokinesis (H,I). Scale bar, 5 µm.

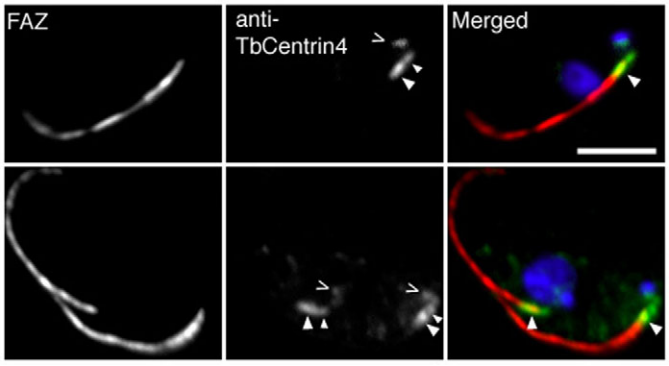

Fig. 7. Association of the bi-lobe with the FAZ. Fixed cells were labeled with L3B2 for FAZ (red), anti-*Tb*Centrin4 for bi-lobe (filled arrowheads; green) and basal bodies (open arrowheads; green), and DAPI for nucleus and kinetoplast (blue). At all stages of the cell cycle, the posterior tip of the FAZ overlapped with the bi-lobe, in particular the anterior lobe (large filled arrowheads). Scale bar, 5 μm.

the cell cycle. This labeling pattern for *Tb*Centrin4 was confirmed by both overexpressing *Tb*Centrin4 fused to fluorescent protein reporters or an epitope tag (Selvapandiyan et al., 2007) and immunofluorescence studies using antibodies raised specifically against *Tb*Centrin4 (this paper). Interestingly, the staining of *Tb*Centrin2 and *Tb*Centrin4 on the basal body and the bi-lobed structure did not completely overlap, perhaps due to difference in abundance or distribution patterns within sub-domains of these organelles.

We have previously shown that RNAi of *Tb*Centrin2 inhibited duplication of basal body, kinetoplast and Golgi. Cytokinesis was also blocked, but nuclear division continued, leading to accumulation of multi-nucleated cells (He et al., 2005). In *Tb*Centrin4-RNAi cells, however, the organelles duplicated normally and cytokinesis proceeded, at least during the early phase of induction (up to 48 hours). Prolonged induction (>48 hours) resulted in a massive disruption of cell-cycle progress and in the accumulation of large multi-nucleated cells, similar to those found using *Tb*Centrin2-RNAi. The major difference, however, was the abundance of zoids in the *Tb*Centrin4-depleted cells, from ~10% at 24 hours post induction to >40% of the cell population at 72 hours. The production of zoids was confirmed by using fluorescence-activated cell sorting and by analyzing siblings for multiple organelles (kinetoplasts, basal bodies, the bi-lobe, Golgi, ERES, mitochondria, lysosomes and flagella). Only the nucleus was found to be absent in the zoids.

Interestingly, these zoids were not observed in earlier studies of *Tb*Centrin4 depletion (Selvapandiyan et al., 2007) but the reasons are unclear. Their absence cannot be attributed to the use of different tetracycline concentrations to induce RNAi or different silencing constructs. Our constructs were generated using RNAit, a widely accepted, web-based tool to select gene-specific fragments for RNAi in *Trypanosoma brucei* (Redmond et al., 2003). However, the same results were obtained when using the fragment selected by Selvapandiyan et al. (Selvapandiyan et al., 2007) (data not shown). It also cannot be explained by an uneven distribution of residual *Tb*Centrin4 because fluorescence analysis using antibodies against endogenous *Tb*Centrin4 showed that >95% of cells lacked this centrin, irrespective of the DNA content. One possibility, however, might be the method used to monitor the DNA content of the parasites. In our experiments cells were centrifuged at 2000 ***g*** for 5 minutes to facilitate adhesion to Alcian-Blue-coated coverslips, a step that might be of particular importance for the smaller zoids if they attach less efficiently because of their size. However, in our hands, the procedure used by Selvapandiyan et al. (Selvapandiyan et al., 2007) gave results that only differed in the number of zoids by 1-2%. The answer might be found in the efficiency of RNAi silencing. Our *Tb*Centrin4-RNAi cells displayed the growth defects at least 24 hours earlier than the cells studied by Selvapandiyan et al. However, without detailed knowledge of the experimental procedures it is not possible to understand why. What is clear is that, under our conditions, zoids are very abundant, constituting more than 40% of the cell population after 72 hours of induction.

The concomitant accumulation of zoids and 1K2N cells at an early stage of induction (24 hours), as well as the frequent observation of unequally dividing cells, suggests that the zoids and 1K2N cells were produced as siblings. Except for the unequal inheritance of the nuclei, all other organelles examined, including basal bodies, kinetoplast, Golgi, lysosomes and flagella, as well as FAZs, were found in both zoids and 1K2N cells and, therefore, appeared to separate normally. Increasing numbers of zoids later in the course of induction suggests that unequal cell division took place even when *Tb*Centrin4 was depleted to <5% of the wild-type level.

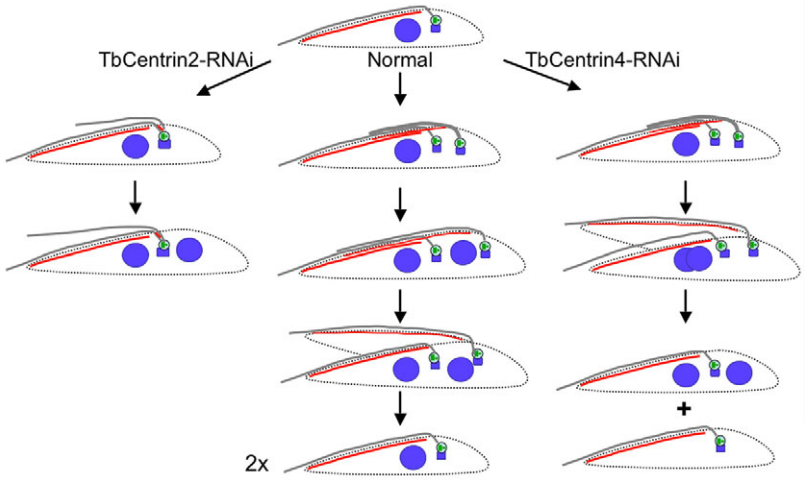

Fig. 8. Model describing the effects of depletion of *Tb*Centrin2 or *Tb*Centrin4. In normal cells (middle), duplication and segregation of basal bodies (green), flagella (gray) and kinetoplasts (small blue squares) are followed by division of the nuclei (large blue circles). Cytokinesis initiates at the anterior end of the cell only after full segregation of the nuclei, with the more-posterior daughter nucleus positioned between the segregated kinetoplasts. The cytokinetic furrow forms in between the segregated organelles and partitions them equally into daughter cells. The FAZ (red) is believed to have an important role in the formation of the cytokinetic furrow. In cells depleted of *Tb*Centrin2 (left), duplication/segregation of basal bodies and kinetoplasts is inhibited, whereas the flagellum and nucleus duplicate normally. Formation of the new FAZ is also inhibited, possibly explaining the subsequent inhibition of cell division. In *Tb*Centrin4-depleted cells (right), duplication and segregation of basal bodies, kinetoplasts, flagella and FAZ appear normal. Nuclear division, however, appears delayed relative to cell division, leading to formation of 1K2N and zoid daughters.

The unequal inheritance of the nuclei was the only obvious defect in *Tb*Centrin4-depleted cells in the early phase of induction and this could arise in several ways. The first is that the cytokinetic furrow could be misplaced, similar to the intraflagellar transport (IFT) mutant identified by Kohl et al. (Kohl et al., 2003). The newly formed FAZ is thought to have a crucial role in cytokinesis by influencing the correct formation of the cytokinetic furrow. The IFT mutant forms a new FAZ that is much shorter than in the control; cytokinesis, therefore initiates much closer to the posterior end, producing one daughter cell that is much smaller than the other. It is interesting to note that the posterior end of the FAZ is partially embedded in the bi-lobe that contains *Tb*Centrin4, and depletion of another bi-lobe component, *Tb*Centrin2, inhibited the formation of new FAZ, possibly explaining why cell division was inhibited in *Tb*Centrin2-deficient cells. However, depletion of *Tb*Centrin4 had no apparent effect on FAZ assembly. The length of the FAZ in zoids and control 1N1K cells were almost identical, consistent with the observation that cytokinesis can occur normally in cells depleted of *Tb*Centrin4.

Another way in which unequal inheritance of daughter nuclei might occur is through inhibition of nuclear division. It is known, for example, that treatment of cells with aphidicolin, an inhibitor of nuclear DNA synthesis, leads to the production of zoids (Ploubidou et al., 1999). So, too, does treatment with the anti-microtubule agent rhizoxin, at a concentration that inhibits nuclear division but not kinetoplast division and cell division (Ploubidou et al., 1999). Inhibition of nuclear division by depletion of mitotic cyclins (Hammarton et al., 2003) or a Cdc2-related kinase (CRK3) can also lead to the production of zoids (Tu and Wang, 2004). However, in cells depleted of *Tb*Centrin4, nuclear division and segregation did occur, albeit perhaps slower than in control cells.

Together, these data suggest that the absence of *Tb*Centrin4 leads to a slower separation of newly formed daughter nuclei, such that cytokinesis leads to the production of zoids and 2N1K cells. This in turn suggests that *Tb*Centrin4 is involved in coordinating the timing of cytokinesis relative to karyokinesis (Fig. 8). In this context, it is interesting to note that overexpression of the *T. brucei* polo-like kinase also generates zoids (Kumar and Wang, 2006), and that this kinase has recently been implicated to function in the duplication of the bi-lobe (deGraffenried et al., 2008). This might provide a possible link to the underlying molecular mechanism of the action of *Tb*Centrin4.

Materials and Methods

Phylogenetic analyses

Protein sequences of centrins and calmodulins were obtained from the following sources: The *T. brucei* protein sequences were obtained from the *Trypanosoma brucei* Genome Project (http://www.tigr.org/tdb/e2k1/tba1). All other sequences were obtained from the Entrez Protein database using the NCBI web site (http://www.ncbi.nlm.nih.gov/sites/entrez?db=protein). GenBank accession numbers for the individual genes are provided in Table 1. Sequences were aligned using MAFFT (Katoh et al., 2005) with settings that provide most accurate alignments (option 'localpair' with a maximum number of 1000 iterations). Coloring of the alignment was done with BOXSHADE implemented in the Biology WorkBench 3.2 (http://workbench.sdsc.edu). Maximum-likelihood sequence trees were reconstructed from the protein-sequence alignment with IQPNNI (Vinh le and Von Haeseler, 2004) using the rtREV-Model of sequence evolution (Dimmic et al., 2002) and 4 Γ-rate categories to model substitution rate variation among sites. Statistical support of branches in the phylogenetic tree was assessed with 100 non-parametric bootstrap replicates. The tree graphic was created with TREEGRAPH (Müller and Müller, 2004). To test for clock-like evolution of the sequences in our dataset, we used the likelihood-ratio clock test implemented in TREEPUZZLE (Schmidt et al., 2002) at a significance level of 5%. Prediction of EF-hand domains in the centrin and calmodulin sequences was done with a HMMER search (http://hmmer.janelia.org) against the SMART database (Letunic et al., 2004) via the ANNOTATOR protein annotation web site (http://annotator.org).

Cell lines

Cells of the procyclic form of the *T. brucei* strain 427 clone 29.13 (Wirtz et al., 1999) were used throughout the study for both recombinant protein expression and RNAi experiments. Cells were maintained in Cunningham medium containing 15% heat-inactivated, TET-system-approved fetal bovine serum (BD Biosciences), supplemented with 15 μg/ml neomycin and 50 μg/ml hygromycin at 28°C.

Plasmids

The full-length *Tb*Centrin4 (Tb927.7.3410) cDNA was fused to the N-terminus of a yellow fluorescent protein (YFP) reporter and stably expressed in *T. brucei* 29.13 cells by using a pXS2 vector (Bangs et al., 1996). A 420 bp fragment (19-438) of the *Tb*Centrin4-coding sequence, selected using RNAit (http://trypanofan.path.cam.ac.uk/software/RNAit.html), an automated, web-based tool for the selection of RNAi targets in *T. brucei* (Redmond et al., 2003), was cloned into the p2T7 vector (Wang et al., 2000) for inducible RNAi. Transfection, selection and cloning were performed as described previously (Djikeng et al., 2004). Expression of double-stranded (ds)RNA was induced using 10, 1 or 0.2 μg/ml of tetracycline (Sigma).

Growth assay

Log-phase cells were diluted to 2×10^5 cells/ml with fresh medium. Cell growth was then monitored every 24 hours, with cells counted using a hemocytometer. The culture was maintained in log-phase (between 1×10^6 and 1×10^7 cells/ml) by dilution. The doubling number was calculated as $\log_2 (N_t\times DF)/N_0$, where N_t is the cell density at each time point, N_0 is the cell density at t=0 or 2×10^5, and DF is the dilution factor.

Polyclonal antibodies

A 6×His tag was fused to the full-length coding sequence of *Tb*Centrin4 and expressed in *E. coli*. Purified 6xHis-*Tb*Centrin4 fusion protein was then injected into rabbits to produce polyclonal antibodies that were subsequently affinity purified. The antibodies were then used for immunoblotting as well as immunofluorescence labeling.

Immunofluorescence microscopy

T. brucei cells were attached to coverslips, fixed and permeablized for 10 minutes with cold methanol at –20°C. The cells were then blocked with 3% BSA in PBS (pH 7.6), followed by incubation with affinity-purified antibodies. Cells were observed using an upright Axioplan2 microscope (Zeiss) equipped with an Orca-II camera and a Plan-Apochromat 100×/1.4-NA DIC objective. Colocalization was detected using an LSM510 confocal microscope (Zeiss). Optical sectionings were performed on a fully automated, inverted Axio Observer microscope (Zeiss) equipped with a Plan-Apochromat 63×/1.4-NA DIC objective. All images were processed using Photoshop software.

Immunoelectron microscopy

Log-phase *T. brucei* cells stably expressing *Tb*Centrin4-YFP were harvested by centrifugation and fixed with 2% paraformaldehyde, 0.2% glutaraldehyde and 0.26M sucrose in 100 mM HEPES pH 7.2, and then further processed for cryo-sectioning. 70-nm-thick cryo-sections were probed with a polyclonal antibody against GFP (Seedorf et al., 1999), followed by protein-A–gold (10 nm) labeling (Department of Cell Biology, University of Utrecht, The Netherlands). Grids were contrasted with 5% uranyl acetate, examined using a Tecnai 12 electron microscope (FEI) and imaged on a Morada 11MPX camera (Olympus).

Flow cytometry and fluorescence microscopy to monitor cell size and DNA content

Cells were fixed with 4% paraformaldehyde for 20 minutes, washed and resuspended in PBS. Fixed cells were stored at 4°C until analysis or sorting. To monitor DNA content by fluorescence microscopy, cells were attached to Alcian-Blue-coated coverslips by centrifugation, permeablized with 0.25% Triton X-100 and then stained with DAPI. To facilitate accurate DNA counting, fluorescence and corresponding DIC images were acquired on randomly selected fields across the coverslips. For each field, we captured a *z*-stack of ten fluorescence optical sections (at 0.5-μm intervals) spanning the entire *T. brucei* cell and one DIC image at the focal plane. The optical sections for each *z*-stack were then collapsed to generate a 2D-projection (similar to the images shown in supplementary material Figs S5 and S6). These 2D images were then viewed together with the corresponding DIC images to ensure correct DNA counting in individual cells.

We thank Jeffrey Salisbury (Mayo Clinic, Rochester, MI) for the 20H5 anti-centrin antibodies and Keith Gull (University of Oxford, UK) for L3B2 antibody. The work was supported by the NIH. I.E. is supported by the Wiener Wissenschafts-, Forschungs-, und Technologiefonds. C.Y.H. is a Singapore National Research Foundation research fellow.

References

Araki, M., Masutani, C., Takemura, M., Uchida, A., Sugasawa, K., Kondoh, J., Ohkuma, Y. and Hanaoka, F. (2001). Centrosome protein centrin 2/caltractin 1 is part of the xeroderma pigmentosum group C complex that initiates global genome nucleotide excision repair. *J. Biol. Chem.* **276**, 18665-18672.

Bangs, J. D., Brouch, E. M., Ransom, D. M. and Roggy, J. L. (1996). A soluble secretory reporter system in *Trypanosoma brucei*. Studies on endoplasmic reticulum targeting. *J. Biol. Chem.* **271**, 18387-18393.

Baum, P., Furlong, C. and Byers, B. (1986). Yeast gene required for spindle pole body duplication: homology of its product with Ca2+-binding proteins. *Proc. Natl. Acad. Sci. USA* **83**, 5521-5516.

Bornens, M. and Azimzadeh, J. (2007). Origin and evolution of the centrosome. In *Eukaryotic Endomembrances and Cytoskeleton: Origins and Evolution* (ed. G. Jékely). New York: Springer-Verlag.

Chapman, M. J., Dolan, M. F. and Margulis, L. (2000). Centrioles and kinetosomes: form, function, and evolution. *Q. Rev. Biol.* **75**, 409-429.

Chen, Y., Hung, C.-H., Burderer, T. and Lee, G.-S. M. (2003). Development of RNA interference revertants in *Trypanosoma brucei* cell lines generated with a double stranded RNA expression construct driven by two opposing promoters. *Mol. Biochem. Parasitol.* **126**, 275-279.

De Graffenried, C. L., Ho, H. H. and Warren, G. (2008). Polo-like kinase is required for Golgi and bilobe biogenesis in *Trypanosoma brucei*. *J. Cell Biol.* **181**, 431-438.

Dimmic, M. W., Rest, J. S., Mindel, D. P. and Goldstein, R. A. (2002). rτREV: an amino acid substitution matrix for inference of retrovirus and reverse transcriptase phylogeny. *J. Mol. Evol.* **55**, 65-73.

Djikeng, A., Shen, S., Tschudi, C. and Ullu, E. (2004). Analysis of gene function in *Trypanosoma brucei* using RNA interference. *Methods Mol. Biol.* **270**, 287-298.

Fischer, T., Rodriguez-Navarro, S., Pereira, G., Racz, A., Schiebel, E. and Hurt, E. (2004). Yeast centrin Cdc31 is linked to the nuclear mRNA export machinery. *Nat. Cell Biol.* **6**, 840-848.

Friedberg, F. (2006). Centrin isoforms in mammals. Relation to calmodulin. *Mol. Biol. Rep.* **33**, 243-252.

Giessl, A., Pulvermuller, A., Trojan, P., Park, J. H., Choe, H., Ernst, O. P., Hofmann, K. P. and Wolfrum, U. (2004). Differential expression and interaction with the visual G-protein transducin of centrin isoforms in mammalian photoreceptor cells. *J. Biol. Chem.* **279**, 51472-51481.

Gogendeau, D., Klotz, C., Arnaiz, O., Malinowska, A., Dadlez, M., de Loubresse, N. G., Ruiz, F., Koll, F. and Beisson, J. (2008). Functional diversification of centrins and cell morphological complexity. *J. Cell Sci.* **121**, 65-74.

Hammarton, T. C., Clark, J., Douglas, F., Boshart, M. and Mottram, J. C. (2003). Stage-specific differences in cell cycle control in *Trypanosoma brucei* revealed by RNA interference of a mitotic cyclin. *J. Biol. Chem.* **278**, 22877-22886.

He, C. Y., Ho, H. H., Malsam, J., Chalouni, C., West, C. M., Ullu, E., Toomre, D. and Warren, G. (2004). Golgi duplication in *Trypanosoma brucei*. *J. Cell Biol.* **165**, 313-321.

He, C. Y., Pypaert, M. and Warren, G. (2005). Golgi duplication in *Trypanosoma brucei* requires Centrin2. *Science* **310**, 1196-1198.

Hu, H. and Chazin, W. J. (2003). Unique features in the C-terminal domain provide caltractin with target specificity. *J. Mol. Biol.* **330**, 473-484.

Hu, K., Johnson, J., Florens, L., Fraunholz, M., Suravajjala, S., Dilullo, C., Yates, J., Roos, D. S. and Murray, J. M. (2006). Cytoskeletal components of an invasion machine-the apical complex of Toxoplasma gondii. *PLoS Pathog.* **2**, 0121-0138.

Katoh, K., Kuma, K., Toh, H. and Miyata, T. (2005). MAFFT version **5**, improvement in accuracy of multiple sequence alignment. *Nucleic Acids Res.* **33**, 511-518.

Klotz, C., Garreau de Loubresse, N., Ruiz, F. and Beisson, J. (1997). Genetic evidence for a role of centrin-associated proteins in the organization and dynamics of the infraciliary lattice in Paramecium. *Cell Motil. Cytoskeleton* **38**, 172-186.

Kohl, L., Sherwin, T. and Gull, K. (1999). Assembly of the paraflagellar rod and the flagellum attachment zone complex during the *Trypanosoma brucei* cell cycle. *J. Eukaryot. Microbiol.* **46**, 105-109.

Kohl, L., Robinson, D. and Bastin, P. (2003). Novel roles for the flagellum in cell morphogenesis and cytokinesis of trypansomes. *EMBO J.* **22**, 5336-5346.

Kumar, P. and Wang, C. C. (2006). Dissociation of cytokinesis initiation from mitotic control in a eukaryote. *Eukaryot. Cell* **5**, 92-102.

Letunic, I., Copley, R. R., Schmidt, S., Ciccarelli, F. D., Doerks, T., Schultz, J., Ponting, C. P. and Bork, P. (2004). .SMART 4.0: towards genomic data integration. *Nucleic Acids Res.* **32**, D142-D144.

Middendorp, S., Kuntziger, T., Abraham, Y., Holmes, S., Bordes, N., Paintrand, M., Paoletti, A. and Bornens, M. (2000). A role for centrin 3 in centrosome reproduction. *J. Cell Biol.* **148**, 405-416.

Müller, J. and Müller, K. (2004). TREEGRAPH: automated drawing of complex tree figures using an extensible tree description format. *Mol. Ecol. Notes* **4**, 786-788.

Page, R. D. M. and Holmes, E. C. (2004). *Molecular Evolution: A Phylogenetic Approach*. p. 209; p. 352. Oxford: Blackwell Publishing.

Paoletti, A., Bordes, N., Haddad, R., Schwartz, C. L., Chang, F. and Bornens, M. (2003). Fission yeast cdc31p is a component of the half-bridge and controls SPB duplication. *Mol. Biol. Cell* **14**, 2793-2808.

Ploubidou, A., Robinson, D. R., Docherty, R. C., Ogbadoyi, E. O. and Gull, K. (1999). Evidence for novel cell cycle checkpoints in trypanosomes: kinetoplast segregation and cytokinesis in the absence of mitosis. *J. Cell Sci.* **112**, 4641-4650.

Redmond, S., Vadivelu, J. and Field, M. C. (2003). RNAit: an automated web-based tool for the selection of RNAi targets in *Trypanosoma brucei*. *Mol. Biochem. Parasitol.* **128**, 115-118.

Robinson, D. R. and Gull, K. (1991). Basal body movements as a mechanism for mitochondrial genome segregation in the trypanosome cell cycle. *Nature* **352**, 731-733.

Robinson, D. R., Sherwin, T., Ploubidou, A., Byard, E. H. and Gull, K. (1995). Microtubule polarity and dynamics in the control of organelle positioning, segregation, and cytokinesis in the trypanosome cell cycle. *J. Cell Biol.* **128**, 1163-1172.

Ruiz, F., Garreau de Loubresse, N., Klotz, C., Beisson, J. and Koll, F. (2005). Centrin deficiency in Paramecium affects the geometry of basal-body duplication. *Curr. Biol.* **15**, 2097-2106.

Salisbury, J. L. (1995). Centrin, centrosomes, and mitotic spindle poles. *Curr. Opin. Cell Biol.* **7**, 39-45.

Salisbury, J. L. (2002). Centrin-2 is required for centriole duplication in mammalian cells. *Curr. Biol.* **12**, 1287-1292.

Salisbury, J. L., Baron, A. and Sanders, M. (1988). The centrin-based cytoskeleton of *Chlamydomonas reinhardtii*: Distribution in interphase and mitotic cells. *J. Cell Biol.* **107**, 635-641.

Schmidt, H. A., Strimmer, K., Vingron, M. and von Haeseler, A. (2002). TREE-PUZZLE: Maximum likelihood phylogenetic analysis using quartets and parallel computing. *Bioinformatics* **18**, 502-504.

Seedorf, M., Damelin, M., Kahana, J., Taura, T. and Silver, P. A. (1999). Interactions between a nuclear transporter and a subset of nuclear pore complex proteins depend on Ran GTPase. *Mol. Cell. Biol.* **19**, 1547-1557.

Selvapandiyan, A., Debrabant, A., Duncan, R., Muller, J., Salotra, P., Sreenivas, G., Salisbury, J. L. and Nakhasi, H. L. (2004). Centrin gene disruption impairs stage-specific basal body duplication and cell cycle progression in Leishmania. *J. Biol. Chem.* **276**, 43253-43261.

Selvapandiyan, A., Kumar, P., Morris, J. C., Salisbury, J. L., Wang, C. C. and Nakhasi, H. L. (2007). Centrin1 is required for organelle segregation and cytokinesis in *Trypanosoma brucei*. *Mol. Biol. Cell* **18**, 3290-3301.

Sheehan, J. H., Bunick, C. G., Hu, H., Fagan, P. A., Meyn, S. M. and Chazin, W. J. (2006). Structure of the N-terminal calcium sensor domain of centrin reveals the biochemical basis for domain-specific function. *J. Biol. Chem.* **281**, 2876-2881.

Sherwin, T. and Gull, K. (1989). The cell division cycle of *Trypanosoma brucei* brucei: timing of event markers and cytoskeletal modulations. *Philos. Trans. R. Soc. Lond., B, Biol. Sci.* **323**, 573-588.

Tu, X. and Wang, C. C. (2004). The involvement of two cdc2-related kinases (CRKs) in *Trypanosoma brucei* cell cycle regulation and the distinctive stage-specific phenotypes caused by CRK3 depletion. *J. Biol. Chem.* **279**, 20519-20528.

Vaughan, S., Kohl, L., Ngai, I., Wheeler, R. J. and Gull, K. (2008). A repetitive protein essential for the flagellum attachment zone filament structure and function in *Trypanosoma brucei*. *Protist* **159**, 127-136.

Vinh le, S. and Von Haeseler, A. (2004). IQPNNI: moving fast through tree space and stopping in time. *Mol. Biol. Evol.* **21**, 1565-1571.

Wang, Z., Morris, J. C., Drew, M. E. and Englund, P. T. (2000). Inhibition of *Trypanosoma brucei* gene expression by RNA interference using an integratable vector with opposing T7 promoters. *J. Biol. Chem.* **275**, 40174-40179.

Wirtz, E., Leal, S., Ochatt, C. and Cross, G. A.(1999). A tightly regulated inducible expression system for conditional gene knock-outs and dominant-negative genetics in *Trypanosoma brucei*. *Mol. Biochem. Parasitol.* **99**, 89-101.

Wolfrum, U., Giessl, A. and Pulvermuller, A. (2002). Centrins, a novel group of Ca2+-binding proteins in vertebrate photoreceptor cells. *Adv. Exp. Med. Biol.* **514**, 155-178.

Yang, A., Miron, S., Duchambon, P., Assairi, L., Blouquit, Y. and Craescu, C. T. (2006). The N-terminal domain of human centrin2 has a closed structure, binds calcium with a very low affinity, and plays a role in the protein self-assembly. *Biochemistry* **45**, 880-889.